Quantitative Comparison of four brain MRI segmentation Techniques

"المقارنة الكمية لاربعة تقنيات في تقسيم صور الرنين المغناطيسي للدماغ "

A. M. Riad[1], Hamdy. K. Elminir, R. R. Mostafa[2]
[1]Head of Information System Department
[2] Faculty of Computer and Information Sciences, Mansoura University
E-mail: amriad2000@mans.edu.eg, reham_2006@mans.edu.eg

ملخص البحث:

تقنية التصوير الرنين المغناطيسي (MRI) تعتبر احدى تقنيات التصوير طبية المتقدمة، التي تساعد في أخذ صور مقطعية داخل جسم الانسان، و تقدم معلومات كثيرة حول الانسجة المختلفة بالدماغ. إن الهدف من تقسيم صور رنين المغناطيسي الخاصة بالمخ هو الفصل بين الانسجة المختلفة الموجوده داخل مخ الانسان للمساعدة في تشخيص الامراض و معالجتها أو التخطيط لعملية جراحية معينة. هناك العديد من الطرق المستخدمة لتقسيم صور المخ. إحدى هذه الطرق هي الطرق التقليدية التي تستخدم تقنيات معالجة الصور التقليدية و التي لا يفضل استخدامها لأنها تحتاج إلى تدخل الإنسان (radiologist) للحصول على الانقسام الدقيق و الموثوق به. من الناحية الأخرى يوجد نوع أخر من الطرق و التي تسمى (unsupervised method) لا تحتاج إلى أي تدخل إنساني (radiologist) و يمكن أن يقوم بتقسم أنسجة الدماغ بدقة عالية. في ضوء هذه الحقيقة، نقوم في هذا البحث بمقارنة أداء أربع طرق لتقسيم الصور في تقسيم صور الرنين المغناطيسي. تعرض النتائج بأن Fuzzy Kohonen's Competitive Learning Algorithms يؤدي بشكل أفضل من ناحية دقة تقسيم الصورة، بينما يؤدي Fuzzy c-means بشكل أفضل من ناحية السرعة في تنفيذ عملية التقسيم.

Abstract

Magnetic resonance imaging (MRI) is an advanced medical imaging technique providing rich information about the human soft tissue anatomy. The goal of brain magnetic resonance image segmentation is to accurately identify the principal tissue structures in these image volumes. There are many methods that exist to segment the brain. One of these, conventional methods that use pure image processing techniques are not preferred because they need human interaction for accurate and reliable segmentation. Unsupervised methods, on the other hand, do not require any human interference and can segment the brain with high precision. In the light to this fact, we in this paper compare the performance of four image segmentation techniques in the subject of brain MR image. Results show that Fuzzy Kohonen's Competitive Learning Algorithms performs better in terms of segmentation accuracy, while FCM performs better in terms of speed of computation.

1. Introduction

Magnetic resonance imaging (MRI) is an important diagnostic imaging technique to obtain high quality brain images in both clinical and research areas because it is virtually noninvasive and it possesses a high spatial resolution and an excellent contrast of soft tissues [1, 2]. MR images are widely used not only for detecting tissue deformities such as cancers and injuries, but also for studying brain pathology [3]. In order to offer useful and accurate clinical information, the segmentation and recognition algorithms of MR images are becoming important subject of the study on medical image processing. Brain tissue segmentation typically classifies voxels into grey matter (GM), white matter (WM), and Cerebrospinal fluid (CSF). Segmentation of MRI is performed manually by trained

Accepted March 1, 2009.

radiologists, but now there are many recent developments are employing to segment the MRI, since manual segmentation of images is a time consuming process and is susceptible to human errors. So there is a need for computer analysis of MRI such as precise delineation of tumors and reliable reproducible segmentation of images.

In segmenting MRI data, we have mainly three considerable difficulties: noise, partial volume effects (where more than one tissue is inside a pixel volume) and intensity in-homogeneity [1]. The majority of intensity in-homogeneities are caused by the irregularities of the scanner magnetic fields–static (B0), radio-frequency (B1) and gradient fields, which produce spatial changes in tissue static. Partial volume effects occur where multiple tissues contribute to a single voxel, making the distinction between tissues along boundaries more difficult. Noise in MR images can induce segmentation regions to become disconnection. Two main reasons lead to the problem of partial volume effects. On the one hand, due to the imaging resolution, the complexity of tissue boundaries causes many voxels to be composed of at least two or more tissues. On the other hand, the constitution of a brain cannot be restricted to only three pure tissues (GM, WM, and CSF). Therefore, it is important to take advantage of useful data while at the same time overcoming potential difficulties [4, 5].

Among many MRI segmentation methods, neural network and fuzzy clustering technique attracted more and more researchers for using it for MRI segmentation.

Neural network attracted more and more researchers for its abilities of parallel operation, self learning, fault tolerance, associative memory, multifactorial optimization and extensibility. But it can not express human expert's knowledge and experience, and the construction of its topological structure lacks of theoretical methods. Moreover the physical meaning of its joint weight is not clear. All these can make the segmentation method of neural networks unstable [4, 6].

Images are by nature fuzzy [7]. This is especially true to the MRI images. The fuzzy property of MRI images is usually made by the limitation of scanners in the ways of spatial, parametric, and temporal resolutions. What's more, the heterogeneous material composition of human organs adds to the fuzzy property in magnetic resonance images (MRI). As the goal of image segmentation is to extract the object from the other parts, segmentation by hard means may despoil the fuzziness of images, and lead to bad results. By contrast, using fuzzy methods to segment MRI images would respect the inherent property fully, and could retain inaccuracies and uncertainties as realistically as possible [8].

There are many research have developed NNs that incorporate fuzzy clustering strategies to overcome the limitation of NN listed above.

The aim of this paper is to implement different techniques of neural network, fuzzy clustering technique, and hybrid approaches to segment brain MRI image. And provide a quantitative comparison of the performance of these image segmentation techniques in subject of brain MR images.

The reminder of this paper is organized as follows. Section 2 description of data used is defined. Section 3 the image segmentation problem is defined .Section 4 present the MRI segmentation techniques. Section 5 gives the result. Finally this paper gives the conclusion in Section 6.

2. Description of data used

Magnetic Resonance Imaging (MRI) and Computed Tomography (CT) are the main sources of 3-D images in medicine. Here, a

brief presentation of the specifics of the MRI acquisition process for brain imaging is given.

When protons in a hydrogen atom (hence in the water within the brain tissues) are placed in a magnetic field, they oscillate with a frequency depending on the strength of the field. They are capable of absorbing energy from the field and when it is switched off they return to their equilibrium by transmitting the absorbed energy.

This re-radiation of energy is observed as the MRI signal. The intensity of a voxel from the MRI data corresponds to averaging the signal over a small area of the brain and over an interval of time. Usually, the tissue area is 1mm2 in the plane (or slice) parallel to the MRI detector. After a slice has been obtained, the detector moves along the third axis to acquire another image. The slice thickness is usually 3 - 5 mm and the gap between slices is usually 2 mm. Therefore, there can be a strongly perceptible difference in the cross-section shape of various anatomical structures between adjacent 2-D slices. The image volumes are obtained by stacking the slices together along the third dimension. The phrase 'third dimension' denotes the axis, along which the resolution is lower. However, the 2-D slices defined along the higher resolution can be physically any of the axes. The 2-D MRI scans can be acquired coronally, sagitally or axially (transaxially) (Figure1), but are all fundamentally 3-D data. An element of a slice is correlated not only to its spatial neighbors within the same slice, but also with spatially adjacent neighbors in nearby slices.

The standard slice orientation is transaxial (or axial) (see Figure 2, left). Slices with sagittal and coronal orientation are shown in Figure 2, middle and right respectively.

The return of the hydrogen nuclei to their equilibrium state takes some time, and is governed by two physical processes.

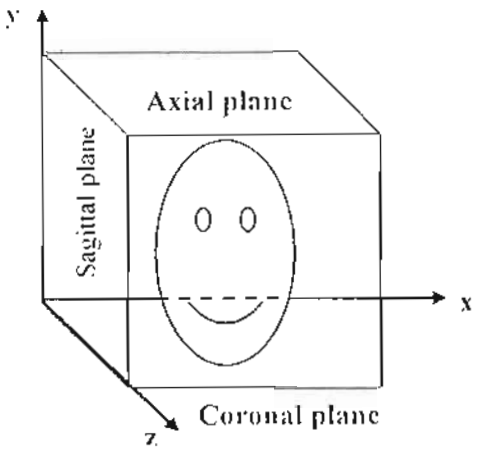

Figure1. MRI plane.

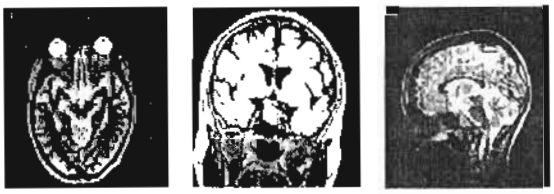

Figure 2. Axial, sagittal and coronal views.

The first is the relaxation back to equilibrium of the component of the nuclear magnetization, parallel to the magnetic field, which takes time T1 and the second is the relaxation of the perpendicular to the magnetic field component which takes time T2. Hence, the strength of the observed MRI signal depends on three main parameters: the Proton Density (PD) in the tissue (The greater the density, the larger the signal), and the times T1 and T2. For most soft tissues in the brain, the proton density is very homogeneous, and therefore does not contribute signal differences to the final image. The times T1 and T2, however, can be dramatically different for various soft tissues, causing major contrast between them in the resulting image. It is possible to manipulate the MRI signal by changing the way in which the nuclei are exposed to the electromagnetic energy. In this way, the dependence of the final MRI image on the three parameters can be specified by weighting techniques.

Figure 3 illustrates the same physical slice of the brain as a PD (left), T1-weighted (middle) and T2-weighted (right) image.

Figure 3. PD, T1 and T2-weighted axial images of a human brain.

When selecting the type of weighting, a tradeoff is made between factors such as cost, time, signal-to-noise ratio, etc. Considerations about the comfort of the patient are also important in this selection. For instance, the T1 images give anatomical details, but tend to be noisy due to the short acquisition time (< 1000 ms for one slice). T2 images possess bigger contrast between the tissues but take longer to acquire (3000 - 4000 ms.). The PD images (typical acquisition time: 2000 ms.), generally manifest the smallest contrast between the tissues. Hence, PD images present the greatest challenges for anatomical segmentation.

3. The image segmentation problem

Image segmentation is a process that partitions an image into the different objects composing it. The objects are sets of points that naturally form a group in their measurement space. In the segmented image, each object is labeled in a way that reflects the "actual structure" of the data and facilitates the description of the original image so that it can be interpreted by the system that handles the image further. Depending on whether spatially separated objects of the same kind have to be labeled the same or not, the image segmentation problem may be regarded as a classification problem or a clustering one, respectively. Several authors (e.g., [4]) employed the following formal definition of image segmentation.

Formal definition: Let F denote the grid of all the pixels in the image, i.e., the set of all the pairs: $F_{N\times M}=\{(i,j)\}: i=1,2,\ldots\ldots N; j=1,2,\ldots\ldots M$. where N and M are the number of rows and columns of the matrix representing the image, and let $P(.)$ be a uniformity (or homogeneity) predicate which assigns the value TRUE or FALSE to a nonempty subset of F, depending only on properties related to the value of the pixels in the subset. $P(.)$ also has the property that given a subset of F, say Y, and a subset of Y, say Z, $P(Y)=TRUE$ implies always that $P(Z)=TRUE$.

A *segmentation* of the grid F for a uniformity predicate P is a partition of F into disjoint nonempty subsets $F_1, F_2, \ldots\ldots F_n$ such that:

(1) $\bigcup_{i=1}^{n} F_i = F$ with $F_i \cap F_j = \phi,\ i \neq j$

(Every pixel must be in one, and only one, segment);

(2) $F_i, i = 1,2,\ldots\ldots n$ is connected

(i.e., composed of contiguous grid points);

(3) $P(F_i)=TRUE$ for $i = 1,2,\ldots\ldots n$

(the segments should be uniform, in terms of the chosen P);

(4) $P(F_i \cup F_j) = FALSE$ when F_i is adjacent to F_j.

In what regards constraint 2) above, the reader familiar with the problem might argue that some of the segmentation algorithms produce nonconnected (or nonconvex) segments (e.g., classical thresholding algorithms). More important, it should be noted that the definition above only defines what are the constraints on a *possible segmentation* of an image, and not what a *correct segmentation* of an image is.

4. Methods

4.1 The Self-organizing Features Map algorithm

With the aim of obtaining adaptive image processing, researchers have tried to employ neural network (NN) approaches. Here, the basic objective is to emulate the human vision processing system which is highly robust and noise insensitive and hence can be applied even when information is ill defined and/or defective/partial.

A self-organizing map (SOM) is a type of artificial neural network that is trained using unsupervised learning to produce a low-dimensional (typically two dimensional), discretized representation of the input space of the training samples, called a map. The map seeks to preserve the topological properties of the input space.

The basic SOFM model consists of two layers. The first layer contains the input nodes and the second one contains the output nodes. The output nodes are arranged in a two dimensional grid.

Every input is connected extensively to every output node via adjustable weights. Let

$X = [x_0, x_1, x_2, \ldots\ldots, x_{N-1}]^t$ be a set of N inputs in R^N such that each x_i has N dimensions (or features).

Let P be the number of output node and $W_j = [w_{0j}, w_{1j}, \ldots\ldots, w_{(N-1)j}]^t$ denote the weights or reference vectors. x_i denotes the input to output node j and w_{ij} is the weight from input node i to the output node j. W_j is the vector containing all of the weights from N input nodes to output node j. Updating weights for any given inputs in SOFM form is done only for output units in a localized neighborhood. The neighborhood is centered on the output node whose distance d_j is minimum. The measurement of d_j is an Euclidean distance, defined as:

$$d_j = \min_j \| x_i - w_{ij} \|^2 \qquad (1)$$

The neighborhood decreases in size with time until only a single node is inside its bounds. A learning rate, $\sigma_{ij}(t)$, is also required which decreases monotonically in time. The weight updating rule is as follows:

$$w_{ij}(t+1) = w_{ij}(t) + \sigma_{ij}(t)(x_i - w_{ij}(t)) \qquad (2)$$

The algorithm works as shown in [9], [10] and [11]. However, SOFM algorithms are, firstly, highly dependent on the training data representatives and the initialization of the connection weights. Secondly, they are very computationally expensive since as the dimensions of the data increases, dimension reduction visualization techniques become more important, but unfortunately the time to compute them also increases. For calculating that black and white similarity map, the more neighbors we use to calculate the distance the better similarity map we will get, but the number of distances the algorithm needs to compute increases exponentially.

4.2 Fuzzy c-means (FCM) for image segmentation

The objective of image segmentation is to divide an image into meaningful regions. Errors made at this stage would affect all higher level activities. Therefore, methods that incorporate the uncertainty of object and region definitions and the faithfulness of the features to represent various objects are desirable.

In an ideally segmented image, each region should be homogeneous with respect to some predicate such as gray level or texture, and adjacent regions should have significantly different characteristics or features. More formally, segmentation is the process of partitioning the entire image into c crisp maximally

connected regions $\{R_i\}$ such that each R_i is homogeneous with respect to some criteria. In many situations, it is not easy to determine if a pixel should belong to a region or not. This is because the features used to determine homogeneity may not have sharp transitions at region boundaries. To alleviate this situation, we can inset fuzzy set concepts into the segmentation process.

In fuzzy segmentation, each pixel is assigned a membership value in each of the c regions. If the memberships are taken into account while computing properties of regions, we obtain more accurate estimates of region properties. One of the known techniques to obtain such a classification is the FCM algorithm [12, 13]. The FCM algorithm is an unsupervised technique that clusters data by iteratively computing a fuzzy membership function and mean value estimates for each class. The fuzzy membership function, constrained to be between 0 and 1, reflects the degree of similarity between the data value at that location and the prototypical data value, or centroid, of its class. Thus, a high membership value near unity signifies that the data value at that location is close to the centroid of that particular class.

The FCM algorithm, also known as Fuzzy ISODATA, is one of the most frequently used methods in pattern recognition.

The FCM algorithm assigns pixels to each category by using fuzzy memberships. Let $X = (x_1, x_2, \ldots\ldots x_N)$ denotes an image with N pixels to be partitioned into c clusters, where x_i represents multispectral (features) data. The algorithm is an iterative optimization that minimizes the cost function defined as follows:

$$J = \sum_{i=1}^{N}\sum_{j=1}^{c} u_{ij}^{m} \| x_i - v_j \|^2 \qquad (3)$$

Where u_{ij} represents the membership of pixel x_i in the ith cluster, v_j is the ith cluster center. $\|.\|$ is a norm metric, and m is a constant. The parameter m controls the fuzziness of the resulting partition, and m =2 is used in this study.

The cost function is minimized when pixels close to the centroid of their clusters are assigned high membership values, and low membership values are assigned to pixels with data far from the centroid. The membership function represents the probability that a pixel belongs to a specific cluster. In the FCM algorithm, the probability is dependent solely on the distance between the pixel and each individual cluster center in the feature domain. The membership functions and cluster centers are updated by the following:

$$u_{ij} = \frac{1}{\sum_{k=1}^{c}\left(\frac{\| x_i - v_j \|}{\| x_i - v_k \|}\right)^{2/(m-1)}} \qquad (4)$$

and

$$v_j = \frac{\sum_{i=1}^{N} u_{ij}^{m} x_i}{\sum_{i=1}^{N} u_{ij}^{m}} \qquad (5)$$

Starting with an initial guess for each cluster center, the FCM converges to a solution for v_j representing the local minimum or a saddle point of the cost function. Convergence can be detected by comparing the changes in the membership function or the cluster center at two successive iteration steps.

4.3 An Adaptive Neuro-Fuzzy System for Automatic Image Segmentation

Auto adaptive neuro-fuzzy segmentation architecture is presented in reference [14]. The system consists of a multilayer perceptron (MLP)-like network that performs image segmentation by adaptive

thresholding of the input image using labels automatically pre-selected by a fuzzy clustering technique. The system's architecture is feedforward, but unlike the conventional MLP the learning is unsupervised. The output status of the network is described as a fuzzy set. Fuzzy entropy is used as a measure of the error of the segmentation system. Given an input image, the system is forced to evolve toward a minimum fuzzy entropy state in order to obtain image segmentation. The system is capable to perform automatic multilevel segmentation of images, based solely on information contained by the image itself. No *a priori* assumptions whatsoever are made about the image (type, features, contents, stochastic model, etc.).

Viewed as a system, the proposed algorithm consists of two main processing blocks (Figure 4): the (fuzzy) error function definition block (A), the adaptive thresholding block (B).

1) Error Function Definition (Block A):

The purpose of this stage is to provide the objective error function to be used by the adaptive thresholding stage. First, the fuzzification block divides the input image into that number of fuzzy sets using FCM, and then the error function definition block generates error function by determining the contribution of each gray level to the fuzzy entropy of the partition.

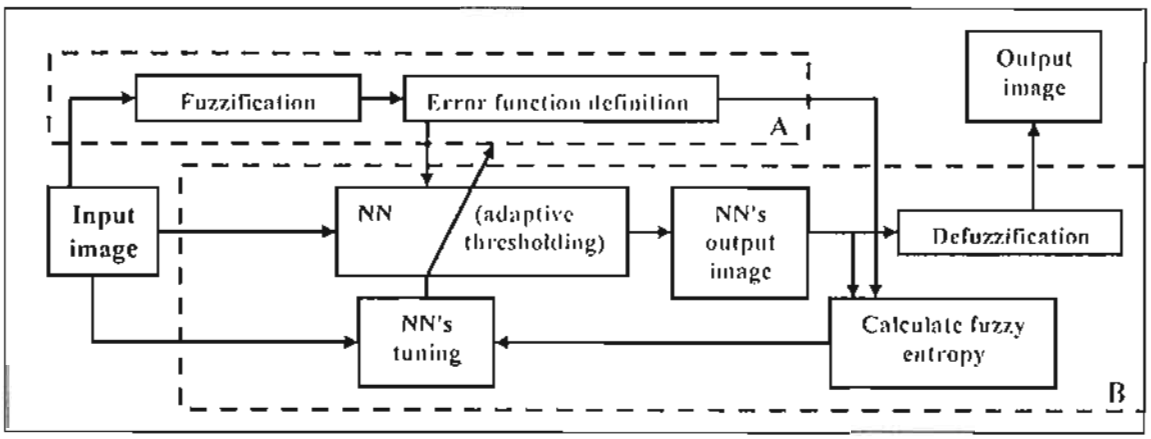

Figure 4. Block diagram of proposed system

2) Adaptive Thresholding (Block B):

This contains the Neural Network (NN) block, the fuzzy entropy calculation block and NN tuning block. Its inputs are the input image and the error function determined by the block (A), and its output is the segmented image.

Neural Network: The neural network block performs adaptive thresholding of the input image. The network architecture consists of an input layer, an output layer and at least one hidden layer. Each layer consists of $M \times N$ neurons, every neuron corresponding to an image pixel.

Activation function: A *multi-sigmoid* activation function was used to allow more than two stable states of the neuron output. The *multi-sigmoid function* is defined as

$$f(x) = \sum_k \left(\frac{v_k - v_{k-1}}{1+e^{-(x-\theta_k)/\theta_0}} + v_{k-1} \right) \times \left[u\left(x - v_{k-1} + d^2\right) - u\left(x - v_k + d^2\right) \right] \qquad (7)$$

where

u step function;

θ_k thresholds;

y_k target level for each sigmoid, will constitute system's labels:

θ_0 steepness parameter;

d size of neighborhood.

The thresholds and the target values are obtained from the error function, as the gray levels with the maximal and with the minimal levels of fuzziness respectively.

Training: The back-propagation algorithm is employed for training. As we apply Input image the neurons in the first layer receives the input, and will apply it to the Linear Combiner and the Activation Function and produce the output, this output will become the input for the neurons in the next layer. So the next layer will feed forward the data, to the next layer. And so on, until the last layer is reached. We compare the desired and actual output compute the error as the difference between desired output and actual output. Once we decided what adjustment we need to do to the neurons in the output layer, we back propagate the changes to the previous layers of the network. Indeed, as soon as we have desired outputs for the output layer, we make adjustment to reduce the error. Adjustment will change weights of the input nodes of the neurons in the output layer. The weights are updated as follows:

$$\Delta w_{ji} = \begin{cases} \eta\left(-\frac{\partial E}{\partial o_j}\right)\frac{\partial o_j}{\partial I_j}o_i & \text{Output layer} \\ \eta\left(\sum_k\left(-\frac{\partial E}{\partial o_k}\frac{\partial o_k}{\partial I_k}w_{kj}\right)\right)\frac{\partial o_j}{\partial I_j}o_i & \text{Other layer} \end{cases} \quad (8)$$

where

I_j Total input to the i-th neuron;

w_{ji} Weight of the link from neuron i in one layer to neuron j in the next layer;

o_i Output of the i-th neuron in the previous layer;

E Error in the network's output (relative to the desired output image)

η Learning rate.

Note: For simplicity we used 1-D indexes in the above equation, the extension to fit the
2-D NN is straightforward.

For a multisigmoid as previously defined

$$\frac{\partial o_j}{\partial I_j} = o_j\left(y_n - y_{n-1} - o_j\right) \quad (9)$$

and the equation of Δw_{ji} become

$$\Delta w_{ji} = \begin{cases} \eta\left(-\frac{\partial E}{\partial o_j}\right)o_j\left(y_n - y_{n-1} - o_j\right)o_i \\ \eta\left(\sum_k\left(-\frac{\partial E}{\partial o_k}\frac{\partial o_k}{\partial I_k}w_{kj}\right)\right)o_j\left(y_n - y_{n-1} - o_j\right)o_i \end{cases} \quad (10)$$

for the output layer and the other layers respectively.

Defuzzification: The output of the neural network is initially obtained in terms of the gray levels, which are then "fuzzyfied" in order to determine the error. In the idle case when the network converges with no error at all (E=0), the outputs have only values who's membership values are "1" or "0," defuzzification is not necessary. When the network does not converge completely (whether stopped intentionally or not), the fuzzification of the output image does not result in merely crisp membership values. The information about the membership values of the pixels might be useful for further processing, depending on the application at hand. If crisp labeling is required, a defuzzification stage must be added. For display purposes, the simplest defuzzification method is thresholding the fuzzy partition, so that each pixel is uniquely assigned to the class in which it has the highest membership value.

4.4 A Fuzzy Kohonen's Competitive Learning Algorithms for MR Image Segmentation

Most brain MRI images always present overlapping gray-scale intensities for different tissues. To overcome this problem, fuzzy methods are integrated with Kohonen's competitive algorithm in Fuzzy Kohonen's Competitive Learning Algorithms (F-KCL) in [15]. The F_KCL algorithm fuses the competitive learning with fuzzy c-means (FCM) cluster characteristic and can improve the segment result effectively.

Conventional Kohonen's competitive learning algorithm

Step 1: Similarity Matching:

The distances between the inputs and the weights are computed as follows:

$$d_i = \|x_i - v_i\| \qquad (11)$$

Step 2: the weight adaptation

The weights from the inputs to the "winner" node (that have the minimum distance) are adapted.

$$w_{ij}(t+1) = w_{ij}(t) + \alpha(t) h_{ij}(t)(x_i - w_{ij}(t)) \qquad (12)$$

with

$$h_{ij}(t) = \begin{cases} 1 & \|x_i - v_i(t-1)\| = \min_{1 \le i \le c} \|x_i - v_i(t-1)\| \\ 0 & \text{If} \end{cases}$$

Otherwise (13)

where

$h_{ij}(t)$ denotes the degree of neuron excitation.

$\alpha(t)$ learning rate of the algorithm are monotonically decreasing functions of time.

$$\alpha(t) = \alpha_0\left(1 - \frac{1}{T}\right) \qquad (14)$$

where training procedure is repeated for the number of steps T which is specified prior.

In F-KCL, the degree of neuron excitation $h_{ij}(t)$ and learning rate $\alpha(t)$ are approximated using FCM membership functions.

$$h_{ij}(t) = \exp\left(t\left(\mu_{ij} - \frac{1}{c}\right)\right) \qquad (15)$$

and

$$\alpha_i(t) = \frac{\alpha_i(t-1)}{\alpha_0 + h_{ij}} \qquad (16)$$

Transparently, the neuron excitation and the learning rate are determined by the membership function, but the $h_{ij}(t)$ in this method will not be too large as the time t increase. It is clearly shows that the learning rate $\alpha(t)$ monotonically decreases to zero as time t increase.

5. Result

The comparison between different techniques listed above in this paper will doing as shown in figure 5.

The MRI image is first segmented using one of the segmentation techniques listed above in this paper. The segmented image is separated into three images corresponding to WM, GM, and CSF. Then these images will be compared to the references image using mean squared error to measure the segmentation accuracy. Fuzzy clustering technique, neural network, and combined system between them is employed to segment MR images in this section. The MR images used in this paper are obtained from the *http://www.bic.mni.mcgill.ca/brainweb*

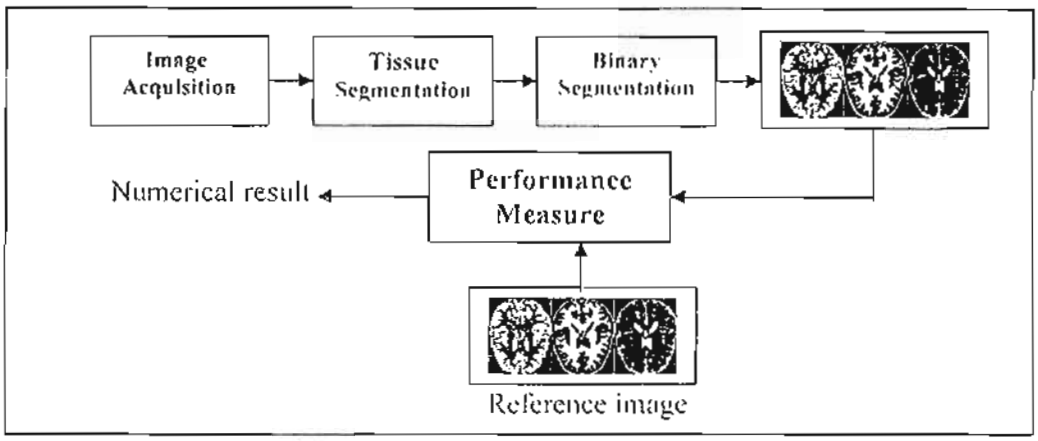

Figure 5. The block diagram of our comparative study process

web site in Montreal Neurological Institute, McGill University. McConnell Brain Imaging Centre (McBIC) [16]. The database is the result of a research work developed at McBIC and contains quantitative 3D investigation of brain structure and function.

The brain phantom and simulated MR images have been made publicly available and can be used to test algorithms such as classification procedures which seek to identify the tissue "type" of each image pixel [17]. The modality, T1-weighted, are downloaded from the website as our experimental data shown in Figure 6. Figure 7 shows the brain MR image Phantoms. They are considered as the true segmented tissues used in this paper.

Figure 6. The planar simulated T1-weghted brain images

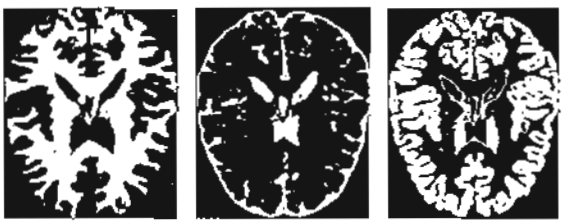

Figure 7. The brain MR image Phantoms

The segmented Grey matter, CSF, and White Matter using SOFM neural network are shown in Figure 8, the segmented images using the Fuzzy c-means are shown in Figure 9, the segmented images using neuro-fuzzy system are shown in Figure 10, the segmented images using a Fuzzy Kohonen's Competitive Learning algorithm are shown in Figure 11.

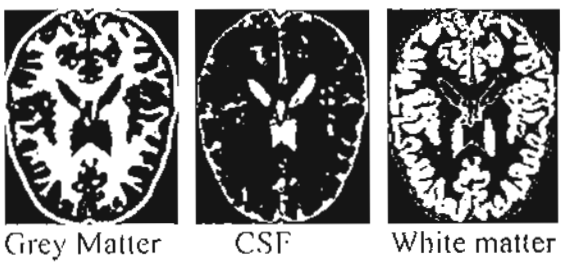

Figure 8. The segmented tissues using SOFM neural network

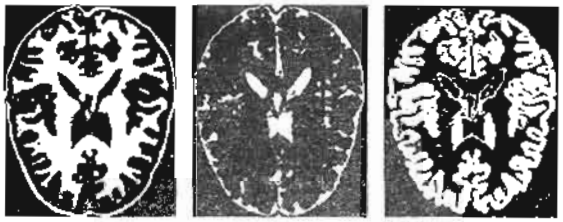

Figure 9. The segmented tissues using Fuzzy c-means

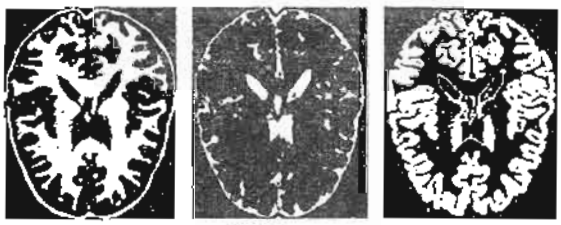

Figure 10. The segmented tissues using neuro-fuzzy system

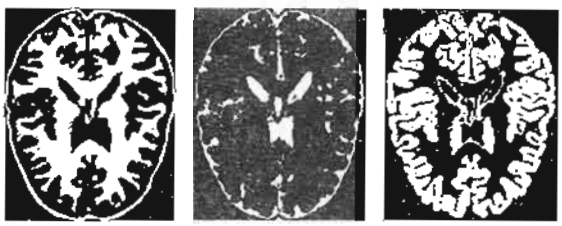

Figure 11. The segmented tissues using Fuzzy Kohonen's Competitive Learning Algorithm

Performance Measure:

An objective method is needed to evaluate the performance of image segmentation algorithms so that different algorithms can be compared. The most important performance criterion is accuracy, that is, the degree to which an algorithm's segmentation matches some reference "gold standard" segmentation.

A number of similarity coefficients are used to specify how well a given segmentation A matches a reference segmentation B, where A and B are sets of segmented pixels.

The binary segmentation of the segmented image were compared with the reference image (Gold standard) by counting the number of correctly classified and misclassified voxel.

The agreement of the binary segmentation with the reference (gold standard) was indicated by the following measures [17]:

1. Similarity Index (SI): is a measure for the correctly classified voxel relative to the total area in both the reference and the area of the segmented image.

$$SI = \frac{2(\mathrm{Ref} \cap Seg)}{\mathrm{Ref} + Seg} \qquad (17)$$

2. Over-Estimated Percentage: measure the area that is falsely classified voxel (Extra) relative to the area of reference image.

$$POE = \frac{\overline{\mathrm{Ref}} \cap Seg}{\mathrm{Ref}} \times 100 \qquad (18)$$

3. Under-Estimated Percentage: measure the area that is falsely not classified voxel (Miss) relative to the area of reference image.

$$PUE = \frac{\mathrm{Ref} \cap \overline{Seg}}{\mathrm{Ref}} \times 100 \qquad (19)$$

4. Correctly-Estimated Percentage: measure the area that is correctly classified voxel (Miss) relative to the area of reference image.

$$PCE = \frac{\mathrm{Ref} \cap Seg}{\mathrm{Ref}} \times 100 \qquad (20)$$

In these definitions, Ref denotes the volume of the reference and Seg is the volume of the binary segmentation (Figure 12). The intersection of Ref and Seg, used

in the SI and PCE. is similar to the volume of the correctly classified voxels (Overlap). The volume of $\overline{Ref} \cap Seg$ corresponds to the false positives (Extra). The volume of $Ref \cap \overline{Seg}$ corresponds to the false negative (Miss). The extra and miss area are shown in Figure 12.

The four image segmentation techniques are implemented on eight T1-wieghted brain MR images that are shown in Figure 13. Table 1 shows the errors between the segmented images using the techniques listed above and the brain MR image Phantoms (Reference image) and the mean of the eight images are reported.

These segmentation techniques were implemented in MATLAB on a PC with Intel Core2Due 2 GHz processor and 3 M RAM.

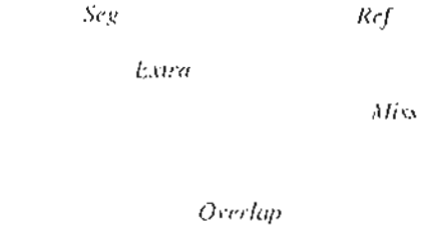

Figure 12: Comparison of a binary segmentation (Seg) with the reference image (Ref), with (Overlap) the correctly classified voxels, (Extra) the false positives and (Miss) the false negatives.

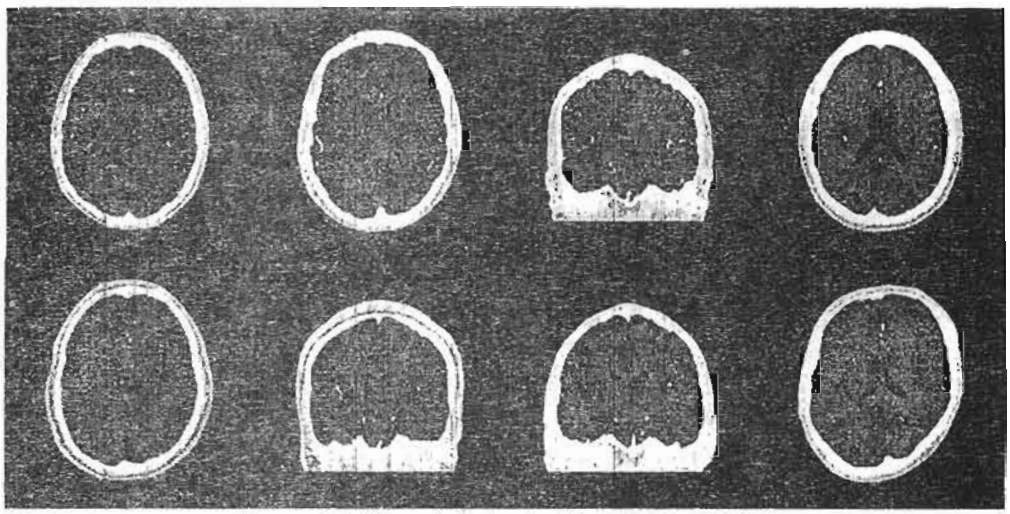

Figure 13: The eight brain T1-wieghted MRI

Table 4.1: The errors between the segmented images and Phantoms

Performance measure / Segmentation technique	SI			POL			PCI			PCE			Time
	GM	CSF	WM	GM	CSF	WM	GM	CSF	WM	GM	CSF	WM	
SOM	87.934	90.120	85.955	10.2	8.5	12.1	11.66	8.966	13.965	88.340	91.034	86.035	44 sec
FCM	90.970	92.532	87.970	8.2	6.3	10.9	8.632	6.666	11.685	91.368	93.334	88.315	35 sec
Neuro-fuzzy system	93.120	95.03	90.943	5.99	4.9	8.89	6.438	4.64	8.875	93.562	95.360	91.125	85 sec
F-KCL	94	98.5	92.5	4.99	0.78	6.75	5.247	2.888	6.776	94.735	97.112	93.224	52 sec

6. Conclusion

Magnetic resonance imaging is commonly employed for the depiction of human soft tissues, most notably the human brain. Computer-aided image analysis techniques lead to image enhancement and automatic detection of anatomical structure.

There are many methods that exist to segment the brain. Of these, conventional methods are

not preferred because they need human interaction for accurate and reliable segmentation which is usually time-consuming and expensive. Unsupervised methods, on the other hand, do not require any human interference and can segment the brain with high precision. For this reason, unsupervised methods are preferred over conventional methods. Many unsupervised methods such as Fuzzy c-means, Self-Organizing map, etc. exist.

Automatic segmentation of MRI volumes of the human brain is a complex task. The clinical acceptance of these methods will greatly depend on the accuracy of the segmentation, ease of computation and the reduction of operator dependence on their performance.

This paper presented an implementation of different intelligent segmentation techniques in the subject of brain MR images. And provide a quantitative comparison between these techniques. Results have shown that F-KCL performs better than other techniques in term of segmentation accuracy and FCM performs better than other techniques in term of speed of computation.

7. References

[1] W. M. Wells, W. E. L. Grimson, and R. Kikins, "Adaptive segmentation of MRI data", IEEE Trans. Medical Imaging, vol. 15, pp: 429-442, 1996.

[2] K. Held, E. R. Kops, and B. J. Krause, " Markov random field segmentation of brain MR images", IEEE Trans. Med. Imag., vol. 16, pp: 878-886, 1997.

[3] M. S. Atkins, and B. T. Mackiewich, "Fully automatic segmentation of the brain in MRI", IEEE Trans. Med. Imag., vol. 17, pp: 98-107, 1998.

[4] L. Jiang, and W. Yang, " A Modified Fuzzy C-Means Algorithm for Segmentation of Magnetic Resonance Images ", VIIth Digital Image Computing, Dec. 2003.

[5] S. Ruan, B. Moretti, J. Fadili, and D. Bloyet, "Fuzzy Markovian,segmentation in application of magnetic resonance images:, Computer Vision and Image Understanding, vol. 85, pp: 54–69, 2002.

[6] Duann, Jung and Makeig: Brain signal Analysis.

[7] J. K. Udupa and P. K. Saha, "Fuzzy connectedness and image segmentation," *Proc. IEEE*, vol. 91, no. 10, pp. 1649–1669, Oct. 2003.

[8] P. K. Saha, J. K. Udupa, and D. Odhner, "Scale-based fuzzy connected image segmentation: Theory, algorithms, and validation," *Compu. Vi. Image Understanding*, vol. 77, pp. 145–174, 2000.

[10] C. A. Parra, K.Iftekharuddin and R. Kozma, "Automated brain data segmentation and pattern recognition using ANN," in the *Proceedings of the Computational Intelligence, Robotics and Autonomous Systems (CIRAS 03)*, December, 2003.

[11] J. Alirezaie, M. E. Jernigan and C. Nahmias, "Automatic Segmentation of Cerebral MR Images using Artificial Neural Networks," in *IEEE Transactions on Nuclear Science*, Vol. 45, No. 4, August, 1998, pp. 2174-2182.

[12] J. C. Dunn, " A fuzzy relative of the ISODATA process and its use in detecting compact well-separated clusters ". Journal of Cybernetics, Vol.3, pp: 32-57, 1974.

[13] J. Bezdek, "A convergence theorem for the fuzzy ISODATA clustering algorithms", IEEE Trans. Pattern Anal. Mach. Intell., 1980.

[14] G. R. Reddy, E. Suresh, S.U. Maheshwar, and M. S. Reddy, " A Neuro-Fuzzy System for Automatic Multi-Level Image Segmentation using KFCM and Exponential Entropy", IFIP International Federation for Information Processing, vol. 228, pp. 367-372,, 2006.

[15] J. Kong, W. Lu, J. Wang, N. Che, and Y. Lu, " A Modified Fuzzy Kohonen's Competitive Learning Algorithms Incorporating Local Information for MR Image Segmentation", IEEE International Conference on Bioinformatics and Bioengineering , pp: 647-653, Oct. 2007.

[16] http://www.bic.mni.mcgill.ca/brainweb: *Simulated Brain Database*, McConnell Brain Imaging Centre, Montreal Neurological Institute, McGill University.

[17] D. L. Collins, A. P. Zijdenbos, V. Kollokian, C. J. Holmes and A. C. Evans, "Design and Construction of a realistic Digital Brain Phantom," in *IEEE Transactions on Medical Imaging*, Vol.,17, No. 3, June, 1998, pp. 463-468.

[18] R. He, S. Datta, B. R. Sajja, and P. A. Narayana, " Generalized fuzzy clustering for segmentation of multi-spectral magnetic resonance images ", Computerized Medical Imaging and Graphics , vol. 32, pp: 353–366, 2008.